DOI: 10.13009/EUCASS2017-258

Multi-Layer Icing Methodologies for Conservative Ice Growth

S. Bourgault-Côté[⋆†], *K. Hasanzadeh*[*], *P. Lavoie*[⋆] *and E. Laurendeau*[⋆†]
[⋆]*Polytechnique Montreal*
C.P. 6079, succ. Centre-ville, Montréal (Qc), Canada, H3C 3A7
[*]*Bombardier*
2351 boul. Alfred-Nobel, Saint-Laurent, Qc, Canada, H4S 2A9
simon.bourgault-cote@polymtl.ca · eric.laurendeau@polymtl.ca
[†]Corresponding authors

Abstract

Three main approaches to the geometrical evolution of ice accretion are presented to discuss the impact of ice mass conservation in ice accretion simulations. An algebraic method, a grid generation method and a level-set method are covered. Each of these methods is developed in two versions, one which is stated as conservative and the other not conservative. First, the iterative version of the algebraic method is conservative. Second, the smoothed grid generation method is globally and locally conservative. Third, the level-set method using the velocity field based on a conserved volume displacement is approaching mass conservation. A verification and a validation of the methods are performed as to compare their behaviour and the effect of ice mass conservation. Verification is performed on a cylinder and a manufactured airfoil with constant ice thickness for each case, showing how some methods handle better than others concave regions and ice thickness strong discontinuities. Validation is done in single- and multi-layer simulations on a glaze ice case and a rime ice case. As expected, conservative methods in multi-layer simulations accord better with the experimental data. In fact, conservative methods allow to reduce the global ice mass error significantly, while local conservation criterion has an effect on the shape of the ice accretion.

1. Introduction

In the context of aircraft design and certification, multiple approaches can be followed to ensure an aircraft is able to safely fly in icing conditions. The demonstration of this result in the modern aeronautic industry requires three main steps: numerical evaluation of ice accretion, wind tunnel experiments and flight tests with simulated ice shapes and in natural icing conditions. This whole certification process is expensive. Thus flight tests are typically left for final confirmation of icing effects and flight worthiness in icing conditions, while wind tunnel experiments with artificial ice shapes are generally limited in numbers and used for validation of numerical simulations during the aircraft design or for development of ice protection systems [Toulouse and Lewis, 2015]. Therefore, only numerical simulations are suitable for a major use in design phases. As the certification regulations are becoming stricter, icing simulations software must be adapted and improved. In reaction, the icing community continuously seek a better modelling of in-flight icing, which is a complex multi-physics problem composed of four main physical phenomena: aerodynamic effects, droplet trajectories and impingement, surface thermodynamic exchanges and geometry evolution.

First generation icing software, which are still in use in the industry, generally consist of a panel method for flow-field simulation, a Lagrangian droplet trajectory module, a thermodynamic Messinger model and a geometric or algebraic method to evolve the geometry. Low computer capacities, compared to nowadays, limited the simulations to be run in two-dimensions. Furthermore, the complexity of performing multi-layer icing simulations in three dimensions also played a role in making two dimensional (2D) simulations attractive, which is still a key factor nowadays. Some methods were then used to combine two dimensional (2D) simulations in order to simulate three-dimensional shapes such as an aircraft [Pueyo, 2013]. Although these software are widely used for aircraft design and certification with success, there is still a need for better modelling algorithms. In the last decades, many developments to achieve this goal have been presented and led to a so-called second generation of icing simulation software which often features a three-dimensional simulation capability [Bourgault et al., 1999, 2000]. A main characteristic of these new software is the

DOI: 10.13009/EUCASS2017-258

replacement of the panel method by a Reynolds Averaged Navier-Stokes (RANS) flow field solver, although first developments regarding this aspect were done in 2D software [Holcomb and Namdar, 1991]. This also introduced a fifth simulation complexity to the whole process by the requirement to mesh the fluid volume instead of only the solid surface. This allowed to replace Lagrangian methods for the droplet trajectories by an Eulerian approach [Bourgault et al., 1999], although it also offers the possibility to simulate Lagrangian trajectories using the fluid mesh in finite volume [Rendall and Allen, 2014]. Without going into details, multiple thermodynamic models and convective heat transfer computation methods have also been studied to improve the modelling of thermodynamic exchanges [Bourgault et al., 2000, Myers, 2001, Zhu et al., 2012].

However, the geometry evolution module is often neglected. In fact, most of the studies specifically dedicated to geometry evolution are considering ice mass conservation only [Thompson et al., 2013] or qualitative criteria to characterize ice accretion [Son et al., 2012]. The latter can be used in a geometry evolution process to ensure a better quality of the ice shape, such as local mass conservation. Yet, such quantitative criteria are difficult to define [RTO/NATO, 2001] and no ideal metric exists for now to the best of the authors knowledge. As for the geometry evolution process, geometric or algebraic methods are still considered as the standard approach to solve for a new geometry, with or without ice mass conservation. The most basic of these methods can be called a normal rectangular evolution, where the surface cells are directly moved normal to the surface. The connections between the new cells are made by various methods, including averaging at bisectors, as in Figure 2(a), or averaging at the intersecting line between moved panels extremities [Son et al., 2012]. This leads to loss or gain of mass depending on the curvature of the geometry. More sophisticated methods use directly the bisectors as limits for a cell evolution and start the process from a known solution, as the icing limits, to obtain a conservative algorithm [Pueyo et al., 2001]. Another conservative 2D variant of the basic algebraic method is to consider the face where the stagnation point is located to move normally to the initial geometry and then to update the other nodes knowing one side of the solution [Fortin et al., 2004]. However, these two last methods are not suited for three dimensional (3D) icing where it is not easy to find the stagnation point, the stagnation line or the icing limits.

For all methods, solving iteratively by evolving the geometry in sub-steps tends to improve the ice mass conservation scheme, as the stretching or shrinking of the panels are considered on a smaller scale, but problems such as geometry folding might arise depending on factors such as geometry curvature and icing time. As the core of the research on the geometry evolution due to ice accretion is still at the algebraic stage, there is a need for better simulation algorithms, specially since algebraic methods are not necessarily expendable from 2D to 3D. To stay in line with the current simulation improvement goal and the possibility to simulate 2D and 3D icing, techniques to move interfaces, instead of nodes, must be studied. For example, [Thompson et al., 2013] proposed a method to evolve a discrete explicit interface by using a face offsetting approach with stabilizer terms to ensure volume displacement conservation and feasibility of the solution. This method also includes an approach to propagate the interface displacement to the volume mesh which was used to compute the ice accretion.

Another path is to use a partial differential equation (PDE) to simulate the evolution of the ice interface. This description applies perfectly to the level-set method, which is a popular numerical tool to identify and track implicit moving interfaces. In fact, it can be described as a PDE equation allowing to track a $(n-1)$–dimensional interface in a n-dimensional space. Recently, Pena et al. [2016] presented a paper where ice accretion is modelled using the well-known level-set equation, but without consideration for the accreted ice mass conservation or for multi-layer requirements, i.e. a compatible geometry for re-meshing or mesh deformation.

This paper presents and discusses geometry evolution methodologies for multi-layer in-flight icing applications with an emphasis on ice mass conservation. First, the classic algebraic non-conservative ice growth method will be presented, followed by the description of three quasi-conservative approaches: an algebraic sub-iteration technique, a grid front method and a level-set method. Second, a verification is performed on a cylinder to ensure the methods ensure mass conservation. The behaviour of the methods in presence of highly concave region will also be presented by the use of a manufactured ice shape. Third, the methods will be compared against experimental data for a rime ice and a glaze ice case. This paper demonstrates the potential of using a quasi-conservative approach compared to standard algebraic methods and aims at opening the discussion on the topic as not much literature is available for icing applications.

2. Aero-Icing Framework

A two-dimensional aero-icing software, NSCODE-ICE [Bourgault-Côté and Laurendeau, 2015], is under development at Polytechnique Montréal since 2012. This software supports the methods presented in this paper. It is composed of five modules: a mesh generation module able to handle complex ice shapes, NSGRID2D [Hasanzadeh et al., 2016], a

DOI: 10.13009/EUCASS2017-258

Reynolds-Averaged Navier-Stokes (RANS) airflow solver, NSCODE [Lévesque et al., 2015], an Eulerian droplet solver [Bourgault-Côté, 2015], a thermodynamic solver [Lavoie et al., 2016] and a geometry evolution solver. NSCODE-ICE is able to perform multi-layer icing and to simulate on overset grids [Lévesque et al., 2015].

Multi-layer ice accretion simulations on airfoils are performed with a decoupled approach by running the five modules sequentially in a loop. Mesh regeneration is performed for each new layer on the accreted geometries. This multi-layer process approximates the unsteady nature of ice accretion with a quasi-steady approach, as the different modules are run in steady mode without contributions from previous simulations except for the wall temperature and the water mass accumulation. Following the assumption that a thin layer of ice does not significantly impacts the solution of the other modules, the quasi-steady assumption is valid. Furthermore, it is expected that the more layers are used, the more the ice shape will converge toward a given solution [Hasanzadeh et al., 2013].

3. Geometry Evolution

3.1 Algebraic Models

Classic Ice growth method: For 2D ice accretion software a typical approach to the ice growth problem is to perform a simple node displacement from the clean surface to the accreted ice. The displacement is dictated by the direction of the ice growth and its magnitude. The most common method is to perform the ice accretion in a direction normal to the body of interest while another approach is to follow the impacting angle of the droplets. The magnitude of the node displacement is generally taken as the mean ice thickness of two neighbouring cells (for 2D simulations), or sometimes a weighted average between the displaced faces extremities [Son et al., 2012]. The process for a classic algebraic model is summarized below.

1. The ice thickness for a node (h_{node}) is computed by averaging the thickness from the 2 neighbouring cells
$$h_{node} = \frac{h_i + h_{i+1}}{2} \tag{1}$$
2. The nodes are moved along the bisectors ($\vec{b}$)
$$\vec{x}_{new} = \vec{x}_{old} + h_{node}\vec{b} \tag{2}$$

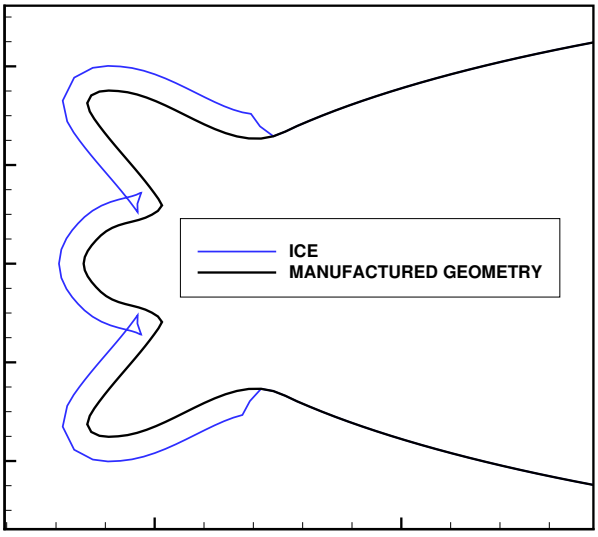

Figure 1: Example of ice intersection on a manufactured case

An important drawback of this so called classic technique is that it is not mass conservative. When the surface is convex, extra mass tends to be created while for concave geometries the ice thickness tends to be underestimated. Figure 2(a) exhibits an example for a convex 2D case. The dashed lines represent the ice growth for a flat surface while the red lines show the ice growth for the curved surface for the cell $i + 1$. Clearly, the volume delimited by the red lines is larger than the volume formed by the dashed lines for the same cell. For the same ice density, the ice volume must

DOI: 10.13009/EUCASS2017-258

be the same whether the surface is flat, convex or concave. Hence to conserve mass, the displacement of the red nodes should be reduced.

Note that displacement conservation can in fact be further defined in two displacement conservation types: linear and volume. The latter is achieved when the volume swept by a moving and deforming face is totally captured by the algorithm. In the case of ice mass, volume displacement conservation is thus required, which cannot be done by moving the nodes in one step when no initial solution is known, such as discussed earlier for methods using the stagnation point location or the icing limits to start the geometry evolution process.

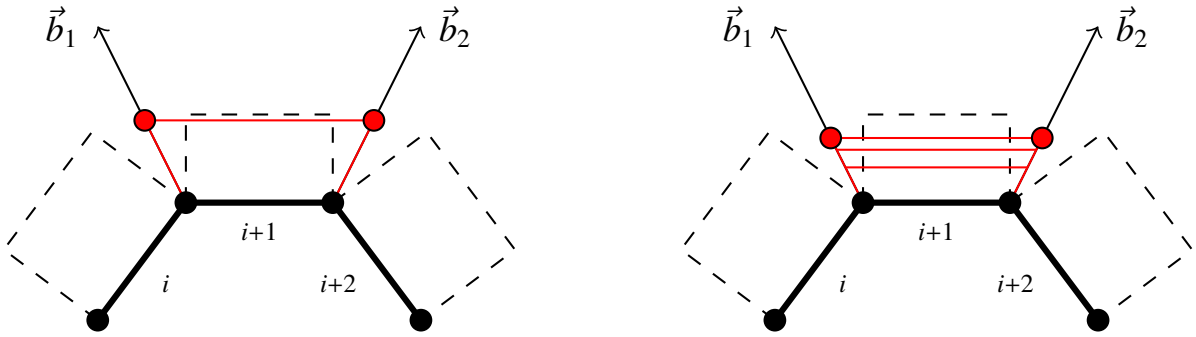

(a) Direct geometry evolution.

(b) Sub-iteration geometry evolution.

Figure 2: Algebraic ice growth on a convex surface: (a) direct (b) sub-iteration

With this classic ice growth method, another issue can occur in highly concave regions where the ice shape can overlap itself, as shown in Figure 1. To solve these issues, an improved geometry evolution scheme is required.

Sub-iteration method: By dividing the ice growth process in sub-iterations, a correction can be applied to account for the surface curvature (convex or concave), which induces stretching or shrinking of the new geometry faces. In fact, this process is comparable to performing a finite integral with n trapeze to compute a volume instead of using only one rectangle. Since intermediate steps are preformed, it also allows the detection and correction of ice intersection (overlapping of the geometry). A special treatment is however required [Ruff and Berkowitz, 1990] which is not straightforward, especially in 3D. The geometry intersection are not handled for the method presented in this paper. The methodology for the sub-iteration method is summarized below.

1. The ice thickness for each sub-layer (noted h_i^0) and at cell i is computed as:
$$h_i^0 = \frac{h_i}{N_{sub}}. \tag{3}$$
where N_{sub} is the total number of sub-iteration and h_i is the overall ice thickness for cell i.

2. For each sub-layer, a correction is applied to account for the change in cell length (ds^n).
$$h_i^n = \frac{h_i^0 ds_i^0}{ds_i^n} \tag{4}$$
where ds_i^0 denotes the initial cell length.

3. The nodes are moved using the usual node displacement method, following the direction of the initial bisectors, see equations (1) and (2).

4. The new curvilinear distance ds_i^{n+1} is evaluated.

5. Step 2 to 4 are repeated until the desired number of sub-layers (N_{sub}) is reached.

If the bisectors were to be updated at each sub-layer, the current description would be sufficient. However, as the approach presented here keeps the initial bisectors, the curvilinear distance ds_i^n must be projected on the initial surface ds_i^0 at each sub-layer.

DOI: 10.13009/EUCASS2017-258

3.2 Grid Models

Normal Grid Line Method: In the realm of structured grid solvers, a preliminary grid approach to evolve the geometry due to ice accretion is to use the already existing normal grid lines of the volume mesh, if such a volume mesh exists. The method is to move the points along the I-constant grid lines, which are normal to the solid surfaces as shown on Figure 3, depending on the ice volume of each solid face. Notably, this offers the possibility to control locally the evolution of the geometry and to apply a local conservation criterion. Furthermore, it does not allow any geometry folding, as the grid lines of the volume mesh should not cross each other.

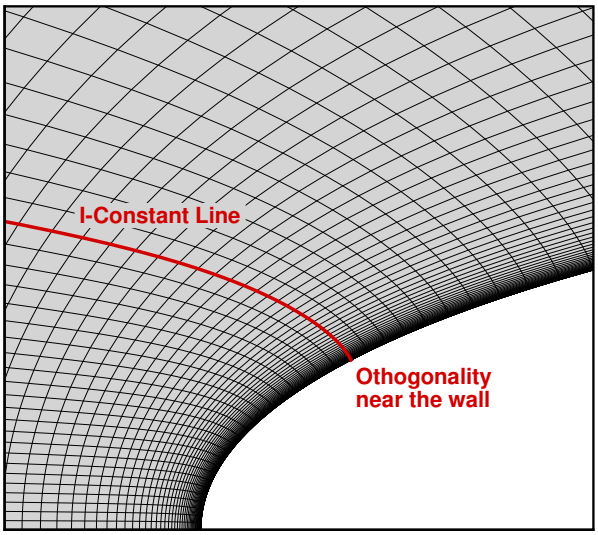

Figure 3: Example of I-constant line as followed for the ice growth process.

Although seeming promising, this method features many drawbacks. First, it cannot be applied to unstructured meshes as the method relies on features from structured grids. Second, as we move away from the geometry, the grid lines are often diverging from the real normal to the geometry as they are the solution to a different problem, specially if the mesh is smoothed. In fact, even the first layer of cells generally do not have a perfect orthogonality at the wall. Third, internal testing in NSCODE-ICE has shown that the final solutions are non smooth and that there is in fact a stiffness in satisfying the local conservation criterion.

Grid Front Method: Instead of purely following the already existing normal grid lines as discussed previously, it is also possible to use grid generation technology to evolve the ice front as an explicit discrete surface. An already existing in-house mesh generation software can be used with some adaptation in this way. Furthermore, this approach can be extended in three dimensions and to unstructured grids. For this paper, the method was implemented into NSCODE-ICE in a module called GridIce2D, as it has been specifically designed for ice accretion simulations.

The method is based on a front marching mesh generation approach with the addition of volume computation for the ice conservation problem. The method also includes an elliptic smoothing that resolve the normals crossing problem and smooth the geometry mesh solution. The methodology is described as follows:

1. Generate two layers of front orthogonal algebraic grids (Figure 4(a));
2. Smooth the mid-layer grid by elliptic equations (Figure 4(b));
3. Use the mid-layer grid to compute the ice volume;
4. Apply the global ice volume conservation criterion;
5. Repeat the process to reduce the volume error to the prescribed value.

The front marching step Δs on each surface node i is computed based on the following equation:

$$\Delta s_i = \frac{2}{n_{iter}} \frac{\Omega_i}{\Delta A_i} \tag{5}$$

DOI: 10.13009/EUCASS2017-258

where Ω_i is the ice volume accumulating on each face i given by the ice accretion solver, ΔA_i is the area of the generated grid face, and n_{iter} is the maximum number of iterations. Note that at each front step, if the global volume conservation error criterion is not reached, the last layer of the grid is regenerated with a halved Δs and this process is repeated to reach the global volume error criteria. Figure 4 shows how the first two steps are done, by first generating algebraic grid layers, and then smoothing the mid-layer grid. Blue dots and lines are numerical constructions only used to compute the iteration smoothed geometry in red.

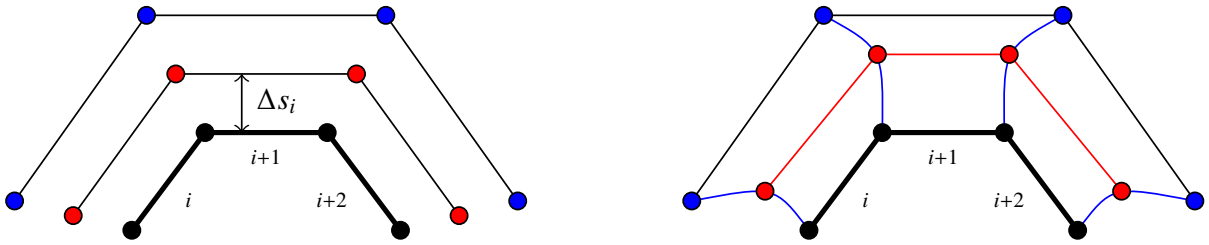

(a) Front orthogonal algebraic grid layers.

(b) Smoothed grid layer (exaggerated).

Figure 4: Front grid ice growth (a) algebraic grid generation step ($L = 1$) and (b) smoothing step.

The front marching structured grid method mainly includes two steps which iteratively generate the grid propagating from the body throughout the domain. The first step is the generation of the algebraic reference grid which includes two local orthogonal grid layers on the base layer.

$$\begin{aligned} \boldsymbol{X}^j_{i,1} &= \boldsymbol{X}^j_{i,0} + \delta^j_i \boldsymbol{n}^j_{i,0} \\ \boldsymbol{X}^j_{i,2} &= \boldsymbol{X}^j_{i,1} + \delta^{j+1}_i \boldsymbol{n}^j_{i,1} \end{aligned} \tag{6}$$

where $\boldsymbol{X}$ is the grid position vector, and $\boldsymbol{n}$ is the normal vector.

The second step is the smoothing of the reference grid layers using the elliptic Poisson equation including stretching and orthogonality control functions which are briefly shown in Eq. (7) in generalized (ξ, η) coordinates.

$$\begin{aligned} g_{22}\left((1+\nu)\,\boldsymbol{X}_{\xi\xi} + P\boldsymbol{X}_{\xi}\right) + g_{11}\left(\boldsymbol{X}_{\eta\eta} + Q\boldsymbol{X}_{\eta}\right) &= 0 \\ g_{11} &= x^2_{\xi} + y^2_{\xi} \\ g_{22} &= x^2_{\eta} + y^2_{\eta} \end{aligned} \tag{7}$$

An additional term $(1 + \nu)$ is added to the elliptic smoothing to improve the handling of the grid lines crossing in concave regions [Thompson and Soni, 2003]. After smoothing the reference grid layers, the middle grid layer is used to generate the next parabolic grid layers.

As the topological mapping between the initial surface discretization and the front grid layers is the same, it is possible to include a local mass conservation criterion to the process. It also allows the direct use of the generated surface mesh for volume mesh regeneration of mesh moving, as the surface topology remains similar. Note that faces without ice mass are forced to remain unmoving, thus leading to possible non physical solutions at the icing limits if the ice thickness is too high.

3.3 Level-Set Method

Modelling: The level-set equation introduced by Osher and Sethian [1988] is a simplification of the Hamilton-Jacobi equation applied to dynamic implicit interfaces. As previously mentioned, it allows to track a moving implicit interface of $(n-1)$–dimensions in a n-dimensions space, which increases the resolution of the interface definition is this additional dimensions is properly discretized, compared to other methods which move directly the $(n-1)$–dimensions interface. It is in fact an Eulerian formulation of the evolution of a function ϕ in a domain, which is chosen as a signed distance function in this paper. This particular type of function features some interesting properties which are beneficial to the level-set simulation, as a unit gradient norm. The level-set equation itself is usually presented in its basic non-conservative form as shown in Eq. (8).

DOI: 10.13009/EUCASS2017-258

$$\frac{\partial \phi}{\partial t} + \mathbf{V} \cdot \nabla \phi = 0 \tag{8}$$

where t is the physical time and $\mathbf{V}$ is the interface velocity field. Although, in this paper, the conservative form of the equation is implemented.

In the context of icing, the velocity field is called icing front velocity and will further be noted as $\mathbf{V}_i$. Considering ice grows normally to a solid, this icing front velocity must be normal to the interface at any point. Its exact value depends on the ice mass accretion rate obtained from the thermodynamic solver. Thus, its exact initial value at the wall is known as stated in Eq. (9).

$$\mathbf{V}_{i,wall} = \frac{\dot{m}_{ice,wall}}{\rho_{ice} \Delta A_{wall}} \cdot \mathbf{n}_{wall} \tag{9}$$

where ρ_{ice} is the ice density, ΔA_{wall} is the area of a surface element on the wall and $\boldsymbol{n} = \nabla\phi / |\nabla\phi|$ is the normal vector to the interface. Pena et al. [2016] suggested that the norm of this wall icing front velocity should be directly propagated normally to the initial geometry. However, as the icing front velocity $\mathbf{V}_i$ contains a local area component ΔA which is the surface element area, its value should also depend on the local cell dimensions. Thus, a first step toward the conservation of ice mass accretion is to ensure the computation of the correct velocity field. In this case, a suggested approach is to propagate the mass accretion rate $\dot{m}_{ice}$ itself in the domain and then to retrieve the icing front velocity as needed with Eq. (10), where ΔA_{local} is a cell characteristic area projected on the interface.

$$\mathbf{V}_{i,local} = \frac{\dot{m}_{ice,local}}{\rho_{ice} \Delta A_{local}} \cdot \mathbf{n}_{local} \tag{10}$$

The two approaches can be classified as conservative, but they do not conserve the same aspect of the interface movement. The propagation of $|\mathbf{V}_i|$ allows to conserve the linear displacement computed at the initial geometry. Thus, the solutions should be similar to the algebraic methods run in a single step. On the contrary, the propagation of $\dot{m}_{ice}$ in the domain allows to conserve the volume displacement of the interface, i.e. the volume swept by the interface during its movement. Thus, if the local linear velocity is retrieved correctly in the domain, the volume cells stretching or shrinking should be considered in the interface displacement. In the context of ice growth, the conservation of ice volume is equivalent to the conservation of ice mass, indicating that this second approach should be selected.

In this paper, solutions for both methods are given. Furthermore, in both cases, the propagation of the main parameter, be it $|\mathbf{V}_i|$ or $\dot{m}_{ice}$, is propagated in the domain using an equation similar to the level-set equation while using directly the normal $\boldsymbol{n}$ as propagation velocity, as it can be seen in Eq. (11) where φ represents the propagated parameter. In this way, a search algorithm is not required and the level-set solver can be reused with little adaptation to solve both equations.

$$\frac{\partial \varphi}{\partial t} + \mathbf{n} \cdot \nabla \varphi = 0 \tag{11}$$

To compare both approaches, Figure 5(a) presents the normal propagation of the wall icing front velocity while Figure 5(b) presents the recovered icing front velocity obtained from the propagated ice mass accretion rate. It can be seen that the linear velocity is properly conserved in the former, which is not the case in the latter as the volume cells are bigger as they are farther away from the geometry. This comparison allows to correctly assess the difference between linear displacement conservation and volume displacement conservation.

Numerical Implementation: The level-set equation model an unsteady phenomenon, thus a proper strategy to solve unsteady equations must be implemented. In this work, the level-set equation is solved using an implicit dual-time stepping scheme with a second-order backward time discretization and a second-order upwind spatial discretization, which are chosen due to the purely hyperbolic nature of the equation. The physical time step used for the temporal integration depends on a Courant-Friedrichs-Lewy (CFL) condition applied before the first level-set integration. This time step is then kept constant during all the level-set simulation.

Note that the initialization of the variable ϕ is done by solving the Eikonal equation, a modified steady form of the level-set equation which features a unit source term [Xia and Tucker, 2010]. The same discretization method as for the level-set equation is applied, again with the same solver which thus solve three different equations. Also, $\nabla\phi$ is recomputed at each movement of the interface, thus adapting the normal to the interface, $\boldsymbol{n}$, and the icing front velocity direction, but the norm of the latter is not re-initialized after each interface movements and neither is the level-set

DOI: 10.13009/EUCASS2017-258

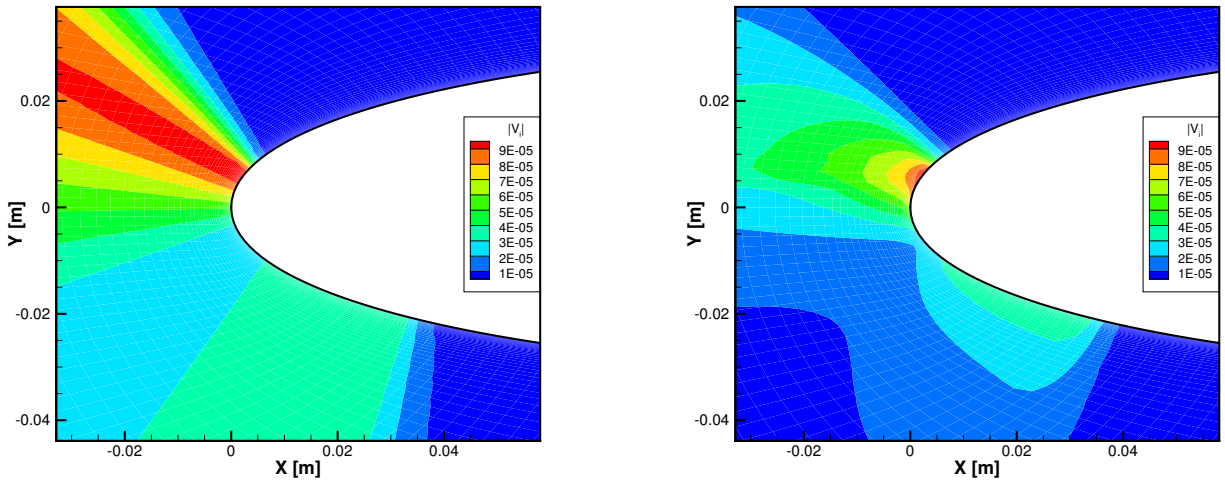

(a) Propagated wall icing front velocity.

(b) Cell dependent icing front velocity.

Figure 5: Icing front velocity obtained from (a) wall surface elements and (b) local volume cells.

variable ϕ itself.

Furthermore, no global nor local volume conservation criterion is applied to reduce the final ice mass error, as the level-set interface evolution is directly related to the physical time. The only aspect allowing to achieve volume or mass conservation is the use of the volume displacement conservative icing front velocity. As the icing front velocity norm and the level-set solution are not re-initialized at each interface movement, full conservation of the ice mass cannot be achieved, which can be considered a limitation of this work, but as the level-set method is not the main focus, this limitation is acceptable.

4. Verification

4.1 Error Computation

The concept of ice mass conservation being the main topic of this paper, a clear quantitative criterion is required. In this work, we consider that a geometry evolution method yielding a relative global ice mass error below 2% is conservative enough for engineering problems such as in-flight aircraft icing. Note that either mass and volume can be used in this context as they are related by a constant in the field, which is the ice density. Also, in most cases, achieving local conservation is a preferred approach, has it allows to conserve the global mass and also the local geometric features of the ice accretion. In the case of local conservation, a local error of less than 5% for all surface elements is judged acceptable for engineering accuracy.

The ice mass errors presented for the verification and validation cases are computed as follow:

$$\epsilon_{ice} = \frac{\Omega_{ice} - \Omega_{ice,0}}{\Omega_{ice,0}} \tag{12}$$

where ϵ_{ice} is the ice mass error, or volume error, Ω_{ice} is the final volume of ice obtained and $\Omega_{ice,0}$ is the predicted volume of ice which should be accreted. This predicted volume of ice is obtained by directly integrating the icing front velocity at the wall with respect to time, as if there was no curvature effects and the cell dimensions were not changing.

4.2 Ice Accretion on a Cylinder

A comparison of the methods is done for a single layer of ice on a cylinder of unit diameter. Furthermore, the ice accretion solution is manufactured to be constant over the left half of the cylinder. The ice mass accretion rate is computed for a $100s$ considering that the ice would reach a height of 0.2 diameter if there was no curvature. Therefore,

DOI: 10.13009/EUCASS2017-258

it is expected that the non-iterative algebraic method and the linear displacement conservative level-set method will both reach this ice height, thus having a high error mass.

The cylinder mesh is made of 257 nodes on the wall and 65 nodes in the other direction, with a farfield located at 5 diameters. This small distance between the farfield and the geometry is possible as only the level-set method is solved on the volume mesh and only cells near the interface are important. As the interface displacement will move up to 0.7 diameter from the origin, the mesh radius of 5 diameters is enough.

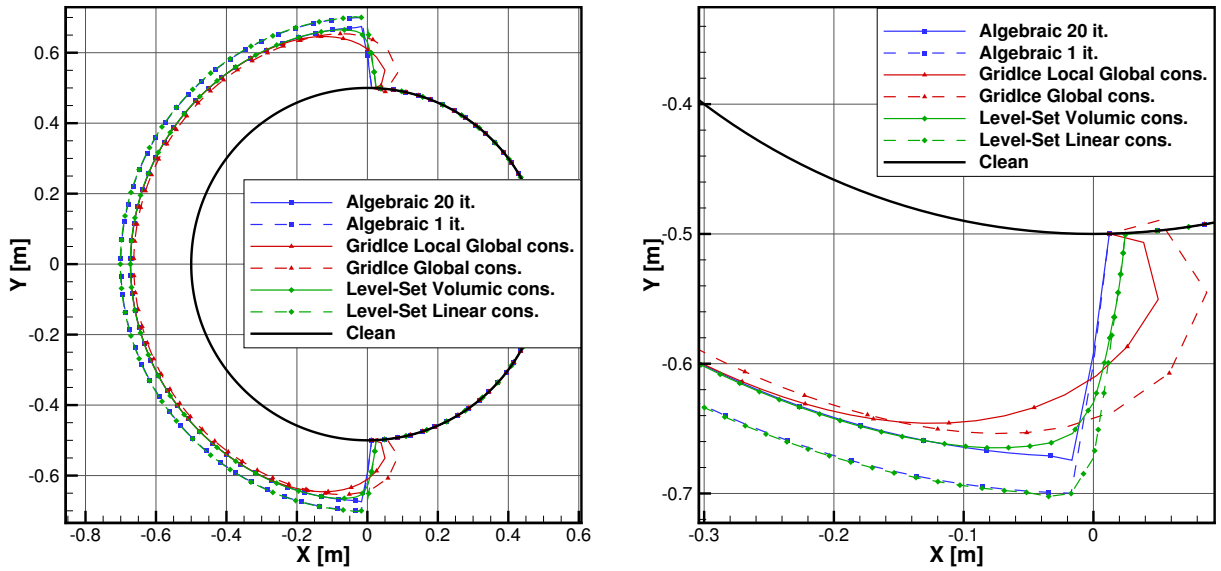

(a) Cylinder ice accretion.

(b) Close view at lower iced limit.

Figure 6: (a) Ice accretion on the cylinder and (b) close view of its lower iced limit.

Figure 6(a) shows the complete view of the half iced cylinder, showing that the conservative methods, namely the sub-iterative algebraic, the volume displacement conservative level-set and the local conservative grid methods, all reach a similar solution in the most part of the ice accretion volume. Similarly, the non-conservative algebraic and the linear displacement conservative level-set reach the same solution, which was expected. In fact, both methods reach a ice height of 0.2 diameter with less than 0.1% error. As for the non local conservative grid method, it is completely different due to fundamental differences in the method, but is still globally conservative, which highlight the importance of local mass or local volume conservation.

The main differences between the methods is highlighted in Figure 6(b), where the algebraic method (iterative or not) show a sharp ice limits modelling, while the level-set method (linear or volume conservative) modelled a smooth interface. The grid method presents an overlapping of the new geometry with the initial one, as the interface node between the iced and the non-iced regions is not allowed to move, which induces a non realistic backward growth. Furthermore, as the topology map stays the same, there is not enough points in this region to properly evolve the geometry with the grid algorithm. The introduction of diffusion in the algorithm might allow the points to be redistributed in this region, but it is important to keep in mind that such a geometry jump is not natural and would not happen in multi-layer icing. The global ice mass errors obtained for each method are listed in Table 1.

4.3 Manufactured Case

The manufactured ice case exhibits three ice horns and was initially created from a NACA0012 airfoil to assess the numerical behaviour of runback water on complex ice geometries [Lavoie et al., 2016, 2017]. The airflow features four recirculation zones. It also exhibits two water accumulation points. The manufactured geometry is also useful to test the ice evolution in the presence of highly convex and concave regions, where the ice growth process is the most critical.

For the verification of the geometry evolution methods, the aerodynamics solver, the droplet trajectories and the thermodynamic balance are not run. Instead, a constant ice thickness is imposed to $0.005m$ (as if the geometry was flat) on the surface elements of the first 15% chord of the airfoil and the geometry evolution solver is run for each method.

DOI: 10.13009/EUCASS2017-258

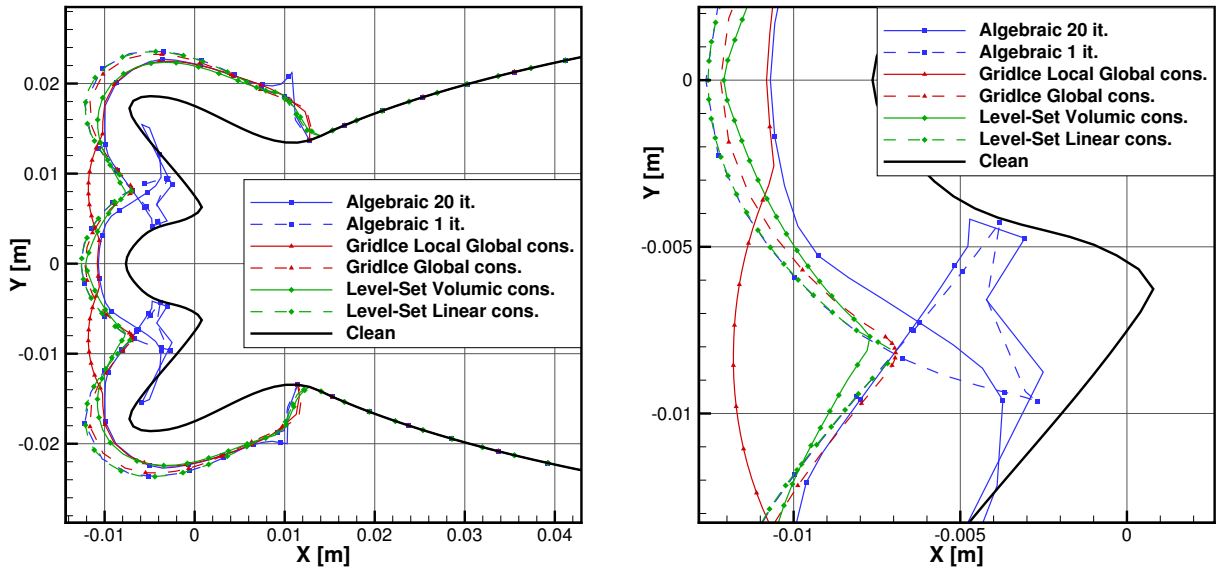

(a) Manufactured airfoil ice accretion.

(b) Close view of the lower concave region

Figure 7: (a) Ice accretion on the manufactured airfoil and (b) close view of its lower concave region.

The icing time associated to the ice mass accretion rate is $100s$, which is important for the level-set solver. The chord of the airfoil is $0.53m$.

Table 1: Ice mass error for the verification cases.

	Cylinder	**Manufactured**
Algebraic 1 it.	15.0%	8.6%
Algebraic 20 it.	−3.4%	−9.7%
Grid global cons.	−0.004%	0.003%
Grid local global cons.	0.006%	0.005%
Level-Set linear cons.	17.2%	5.7%
Level-Set Volume cons.	−2.3%	−8.4%

The results are illustrated in Figure 7 where it can be seen that the algebraic methods cannot solve this problem, yielding strongly overlapping geometries. On the contrary, both the level-set method and the grid method allow to model a correct geometry. However, the local conservation criterion of the grid method gives a different type of result in the concave region, with convex bumps appearing, as it forces the ice to accumulate where it should.

The global ice mass errors obtained for each method are listed in Table 1. From the volume error values, it seems that algebraic methods are similar to level-set results and it is the case for the cylinder case, but the algebraic methods resulted in non physical results on the manufactured case with negative volumes. Thus, the global errors for the algebraic methods on the manufactured case are invalid and cannot be used. Note that the global error with both grid methods is very low as the front marching step is reduced iteratively depending on the global error until the prescribed error value is obtained. However, the resulting ice shape is different when local conservation is not active as ice mass, or volume, is accumulated at any location without any local curvature effect consideration, although it is unknown which ice shape is the more realistic as no experimental data exist on this geometry.

In the case of the level-set approach, the use of the volume displacement conservation allows to better handle the concave regions. As the volume cells are reduced due to concavity in these regions, the icing front velocity increases, as shown in Eq. (10). In turn, in convex regions, the icing front velocity is reduced. The combination of these acceleration and deceleration can be seen on Figure 7(b), as the level-set volume conservative result presents a different final ice height in the concave region than in the convex region, thus effectively flattening the concave region as it would happen in experiments. The still high error is due to missing parts in the implementation of the level-set method, such as the re-initialization of the level-set variable ϕ and of the icing front velocity norm $|\mathbf{V}_i|$ during the interface displacement. These parts are particularly important when dealing with highly concave regions, as the level-set gradient, which define the local normal to the interface, is more complex in such regions. Although the linear displacement conservative variant

DOI: 10.13009/EUCASS2017-258

seems to give a lower absolute error, it is only due to a compensation to the loss mass from bad concave region handling stemming from ice mass gain due to the linear conservation scheme.

5. Validation

In this section, the geometry evolution methods are compared against experimental data from Wright and Rutkowski [1999]. A rime ice (405) and a glaze ice (401) cases are selected with the parameters presented in Table 2. The following results are presented using a RANS solver with the Spalart-Allmaras turbulence model and the Boeing roughness extension [Aupoix and Spalart, 2003]. The convective heat transfer coefficient is computed from the solution of the RANS equations by imposing an isothermal wall boundary condition. The droplet cloud is modelled by a mono-dispersed size of droplets and the Iterative Messinger model of Zhu et al. [2012] is used for the heat and mass balance.

Table 2: Parameters for the validation

	401	**405**
Geometry	NACA0012	
Chord $[m]$	0.53	
AoA $[^\circ]$	3.5	
Velocity $[m/s]$	102.80	
Static Temperature $[K]$	265.37	250.37
Static Pressure $[kPa]$	100.0	
LWC $[g/m^3]$	0.55	
MVD $[\mu m]$	20.0	
Icing Time $[s]$	420.0	
Roughness (k_s) $[\mu m]$	756.5	312.9

Figure 8(a) presents the comparison of the results obtained for 1 layer of glaze ice, while Figure 8(b) presents the results for 10 layers of glaze ice, i.e. for case 401. Figures 9(a) and 9(b) present the same comparisons for case 405 for 1 layer and 10 layers of rime ice respectively.

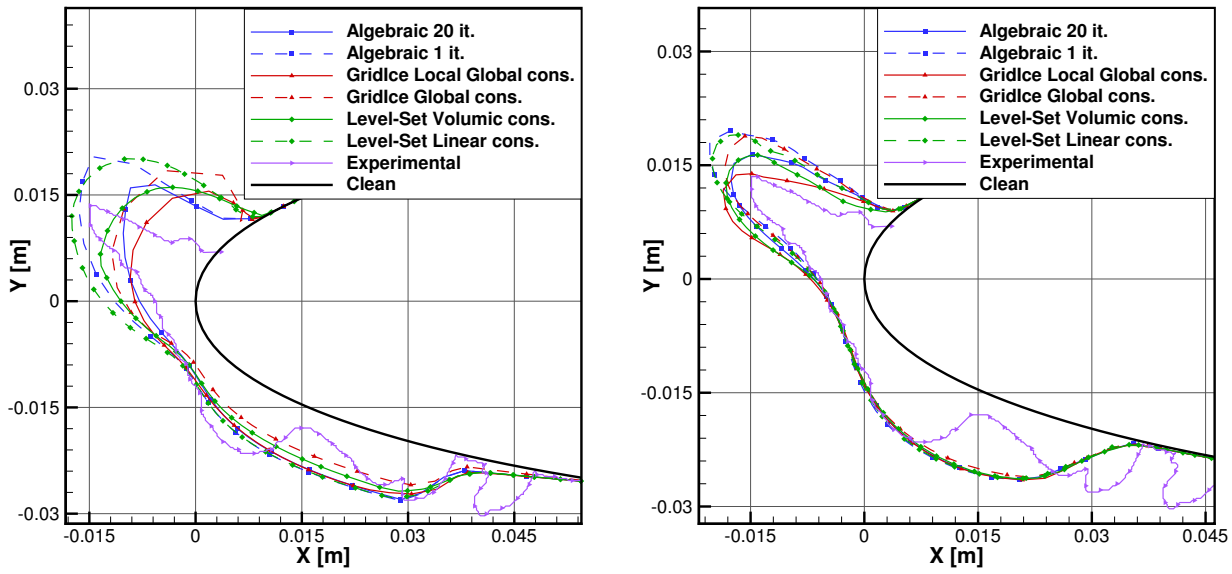

(a) 1 layer

(b) 10 layers

Figure 8: Comparison of the geometry evolution methods for Case 401 on (a) 1 layer (b) 10 layers

The ice mass errors for each method and every cases in single- and multi-layer are listed in Table 3. Note that for the multi-layer results, the predicted ice volume used to compute the error is a summation of the volume predicted at each layer, but the final ice volume is computed for the last layer only. This allows to compute a global error of the whole process and also includes errors coming from the re-meshing and redistribution of surface nodes.

DOI: 10.13009/EUCASS2017-258

Figure 9(a) presents the comparison of the results obtained for 1 layer of rime ice, while Figure 9(b) presents the results for 10 layers of rime ice, i.e. for case 405.

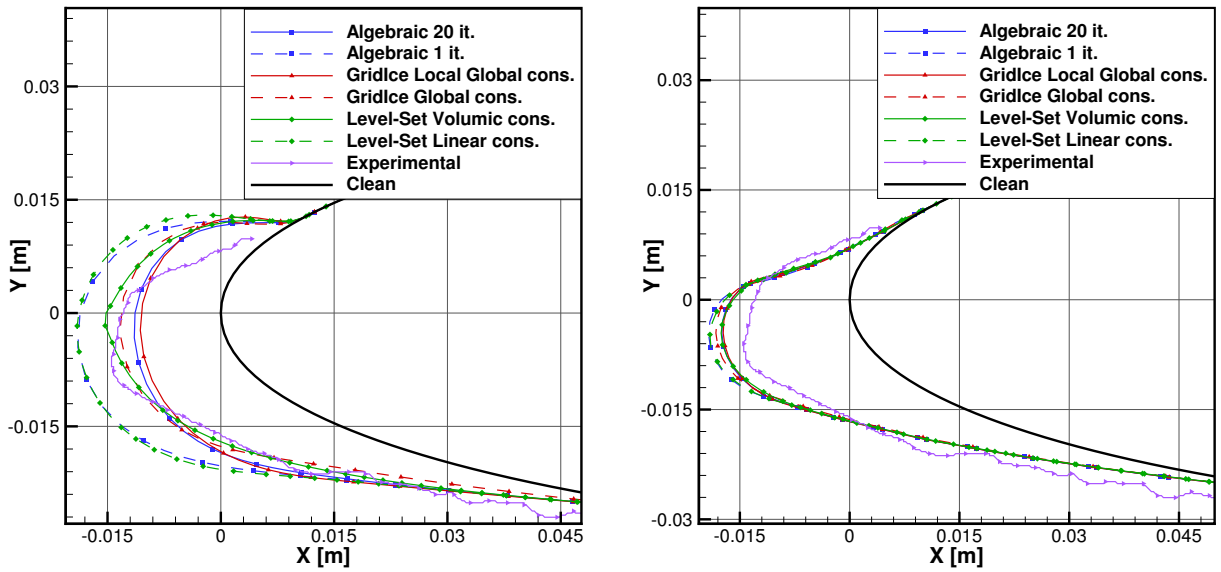

(a) 1 layer

(b) 10 layers

Figure 9: Comparison of the geometry evolution methods for Case 405 on (a) 1 layer (b) 10 layers

Table 3: Ice mass error for the validation cases.

	401 – 1 layer	**401 – 10 layers**	**405 – 1 layer**	**405 – 10 layers**
Algebraic 1 it.	30.0%	5.9%	41.7%	4.7%
Algebraic 20 it.	0.6%	0.000%	0.8%	0.042%
Grid global cons.	−0.007%	0.001%	−0.004%	−0.002%
Grid local global cons.	0.005%	0.001%	0.001%	−0.002%
Level-Set linear cons.	42.2%	5.8%	47.6%	4.3%
Level-Set Volume cons.	7.8%	0.7%	5.5%	−0.9%

In Table 3, it can be seen that performing multi-layer simulations allows to reduce the global ice mass error. Furthermore, using a conservative geometry evolution scheme allows to reduce this error by an order of magnitude. In fact, it can be noted that combining both approaches lead to an error reduced by two orders of magnitude. Also, the local conservative criterion effect is not visible in the global mass error, but this effect can be seen on the ice shapes presented in Figures 8 and 9. The level-set method error is higher than the other methods as it is not fully conservative, the icing front velocity and the level-set variables not being re-initialized during the interface evolution process.

The error obtained with the single iteration algebraic method is similar to the one obtained with the level-set method with linear displacement conservation, which was expected from results in the verification section. However, the difference is higher when comparing the errors of the 20 iterations algebraic and the volume displacement conservative level-set methods, even if visually the ice shapes are similar.

6. Discussion

A verification and a validation of the methods were performed as to compare their behaviour. In the verification section, recall that the first case is a cylinder on which a constant ice thickness was imposed on half of its surface. The simple algebraic method and the level-set with conservation of the linear displacement provide very similar results, as they are both non conservative in term of ice volume. The conservative approaches are also equivalent on this simple case. Differences occur near the point where the ice thickness turns to 0. The two variants of the algebraic method provide a sharp interface, the level-set methods are more diffusive thus leading to a smoother transition to $h = 0$. The grid method is also smoother in this region but provide a non physical behaviour since the last point cannot move as a diffusive scheme was not used, leading to a backward ice growth.

DOI: 10.13009/EUCASS2017-258

The second case presented is a manufactured ice shape with highly concave regions and constant ice height imposed on the leading edge section. The algebraic methods resulted in geometry crossing, which is a known problem with this method. However, the grid and level-set methods succeed in generating a smooth ice shape without intersections or overlapping. Furthermore, the locally conservative grid generation method present a flattened ice shape section as the ice which should have been accumulated in the concave regions was forced to accumulate there, thus pushing the front farther than on the convex regions. A similar phenomenon was obtained with the level-set method using the conservative volume displacement approach, but some limitations in the implementation yield in a less apparent flattening. The methods are fairly equivalent elsewhere on the manufactured geometry.

A validation is performed on a glaze ice and a rime ice case. It shows that the use of volume conservation allows to improve the solutions when only one ice layer is performed, as the accreted mass is visually more similar to experimental data. However when adding ice layers (multi-layer process), the conservative methods compare quite well with the experimental ice shape, whereas non-conservative method still have too much volume.

It is observed that the thicker the ice and the more curved the surface, the use of conservative ice growth becomes more important. Furthermore, multi-layer error reduction effect is combined to conservative scheme effects to allow a very low ice mass error (below 1%). In fact, the multi-layer process allows to reduce the errors by one order of magnitude, as does the use of a conservative scheme, and when the effect is doubled when these two features are combined. Therefore, non-conservative schemes, such as the simple single iteration algebraic method, could be used in most simple cases when combined with enough layers of ice as the mass error would then be acceptable.

7. Conclusion

Three main approaches to the geometrical evolution of ice accretion were presented. An algebraic method was covered first, in which the nodes are moved according to the ice thickness in the direction normal to the surface. An alternative approach was presented to allow a quasi-conservation of the ice volume by the use of sub-iterations to grow the ice. Both techniques are not capable of handling geometry crossing (overlapping) if no special treatment is applied.

Then, a method based on the properties of grids was suggested. At first, it was discussed to perform the ice accretion process following the I-constant grid lines, which are normal to the solid surfaces. A more general alternative approach is to directly employs mesh generation methodologies for the ice accretion. Local and global mass conservation criteria can be implemented and used to control the smoothing process of the surface grid generation.

Finally, an Eulerian approach using a level-set method was described. The method automatically deals with geometry crossing, but does not conserve the ice volume if the external velocity field moving the interface is not well chosen. A first approach is to conserve the linear displacement from the wall in the field, while a second approach is to conserve the volume displacement from the wall in the field while retrieving the local linear displacement with local cell dimensions. The latter is a first step toward ice mass conservation. This method also generates a smooth ice geometry.

A verification and a validation of the methods were performed as to compare their behaviour. As verification, constant ice growth on half of a cylinder and on a manufactured airfoil were tested, highlighting advantages and disadvantages of the methods. Then, two validation cases, one rime ice case and one glaze ice case, are presented and compared to experimental results with fair agreement in most cases.

Globally, in the verification and validation cases, the use of global volume conservation allows to significantly reduce the ice mass error obtained with non-conservative schemes and the effect is increased when also using a multi-layer process. Also, the impact of the local conservation criterion in the grid method allows to obtain ice shapes in good agreement with the experimental data in the glaze ice case, suggesting that local conservation has a more significant impact when the global shape of the iced airfoil is largely deformed, such as with glaze ice horns. The level-set method has shown higher ice mass errors in almost all cases, which is due to the non re-initialization of the icing velocity norm and the level-set variable during the interface evolution, which is still a limitation of the implementation.

Future research should cover full three dimensional geometries and challenges related to unstructured ice accretion. The application of a local conservation criterion on the level-set method and the impact of the re-initialization of the icing front velocity norm should also be studied.

DOI: 10.13009/EUCASS2017-258

8. Acknowledgements

This work is supported by Bombardier and the National Sciences and Engineering Research Council of Canada (NSERC).

References

B. Aupoix and P.R. Spalart. Extensions of the Spalart-Allmaras turbulence model to account for wall roughness. *International Journal of Heat and Fluid Flow*, 24(4):454 – 462, 2003. doi: 10.1016/S0142-727X(03)00043-2.

Y. Bourgault, W. G. Habashi, J. Dompierre, and G. S. Baruzzi. A finite element method study of eulerian droplets impingement models. *International Journal for Numerical Methods in Fluids*, 29:429–449, 1999. doi: 10.1002/(sici)1097-0363(19990228)29:4<429::aid-fld795>3.0.co;2-f.

Y. Bourgault, H. Beaugendre, and W. G. Habashi. Development of a shallow-water icing model in FENSAP-ICE. *Journal of Aircraft*, 37(4):640–646, 2000. doi: 10.2514/6.1999-246.

S. Bourgault-Côté and E. Laurendeau. Two-dimensional/infinite swept wing ice accretion model. In *53rd AIAA Aerospace Sciences Meeting*. AIAA Paper 2015-535, January 2015. doi: 10.2514/6.2015-0535.

Simon Bourgault-Côté. Simulation du givrage sur ailes en flèche par méthodes RANS/Eulérienne quasi stationnaires. Master's thesis, Polytechnique Montréal, Montréal, May 2015.

G. Fortin, A. Ilinca, J.-L. Laforte, and V. Brandi. New roughness computation method and geometric accretion model for airfoil icing. *Journal of Aircraft*, 41(1):119–127, 2004. doi: 10.2514/1.173.

K. Hasanzadeh, E. Laurendeau, and I. Paraschivoiu. Quasi-steady convergence of multi-steps navier-stokes icing simulations. *Journal of Aircraft*, 50(4):1261–1274, 2013. doi: 10.2514/1.C032197.

K. Hasanzadeh, E. Laurendeau, and I. Paraschivoiu. Grid-generation algorithms for complex glaze-ice shapes Reynolds-Averaged Navier-Stokes simulations. *AIAA Journal*, 54(3):847–860, 2016. doi: 10.2514/1J054076.

J. E. Holcomb and B. Namdar. Coupled LEWICE/navier-stokes code development. In *29th AIAA Aerospace Sciences Meeting*. AIAA Paper 1991-804, January 1991. doi: 10.2514/6.1991-804.

P. Lavoie, D. Pena, Y. Hoarau, and E. Laurendeau. Comparison of thermodynamic models for ice accretion on airfoils. In *51st 3AF International Conference on Applied Aerodynamics*. 3AF, April 2016.

P. Lavoie, E. Laurendeau, D. Pena, and Y. Hoarau. Comparison of thermodynamic models for ice accretion on airfoils. *International Journal of Numerical Methods for Heat and Fluid Flow*, 2017. doi: 10.1108/HFF-08-2016-0297.

A. T. Lévesque, A. Pigeon, T. Deloze, and E. Laurendeau. An overset grid 2D/infinite swept wing URANS solver using recursive cartesian bucket method. In *53rd AIAA Aerospace Sciences Meeting*. AIAA Paper 2015-912, January 2015. doi: 10.2514/6.2015-0912.

T. G. Myers. Extension to the messinger model for aircraft icing. *AIAA Journal*, 39(2):211–218, 2001. doi: 10.2514/2.1312.

Stanley Osher and James A Sethian. Fronts propagating with curvature-dependent speed: Algorithms based on hamilton-jacobi formulations. *Journal of Computational Physics*, 79(1):12 – 49, 1988. ISSN 0021-9991. doi: 10.1016/0021-9991(88)90002-2.

Dorian Pena, Yannick Hoarau, and Eric Laurendeau. A single step ice accretion model using level-set method. *Journal of Fluids and Structures*, 65:278 – 294, 2016. ISSN 0889-9746. doi: 10.1016/j.jfluidstructs.2016.06.001.

A. Pueyo. Efficient 3D artificial ice shapes simulations with 2D ice accretion codes using a 3-level correction. In *SAE 2013 AeroTech Congress and Exhibition*, volume 7. SAE Technical Paper 2013-01-2136, September 2013. doi: 10.4271/2013-01-2136.

A. Pueyo, D. Chocron, and F. Kafyeke. Improvements to the ice accretion code CANICE. In *8th CASI Aerodynamics Symposium*. CASI, May 2001.

DOI: 10.13009/EUCASS2017-258

T.C.S. Rendall and C.B. Allen. Finite-volume droplet trajectories for icing simulation. *International Journal of Multiphase Flow*, 58:185 – 194, 2014. ISSN 0301-9322. doi: 10.1016/j.ijmultiphaseflow.2013.08.007.

RTO/NATO. Ice accretion simulation evaluation test. Technical report, North Atlantic Treaty Organization, November 2001.

G. A. Ruff and B. M. Berkowitz. Users manual for the NASA Lewis ice accretion prediction code (LEWICE). Technical Report CR 185129, NASA, 1990.

C. Son, S. Oh, and K. Yee. Quantitative analysis of a two-dimensional ice accretion on airfoils. *Journal of Mechanical Science and Technology*, 26(4):1059–1071, 2012. doi: 10.1007/s12206-012-0223-z.

D. Thompson, C. Tong, Q. Arnoldus, et al. Discrete surface evolution and mesh deformation for aircraft icing applications. In *5th AIAA Atmospheric and Space Environments Conference*. AIAA Paper 2013-2544, June 2013. doi: 10.2514/6.2013-2544.

D. S. Thompson and B. K. Soni. ICEG2D: A software package for ice accretion prediction. In *41st AIAA Aerospace Sciences Meeting and Exhibit*. AIAA Paper 2003-1070, January 2003. doi: 10.2514/6.2003-1070.

Marie-Laure Toulouse and Richard Lewis. A350XWB icing certification overview. In *SAE 2015 International Conference on Icing of Aircraft, Engines, and Structures*. SAE Technical Paper 2015-01-2111, June 2015. doi: 10.4271/2015-01-2111.

W. B. Wright and A. Rutkowski. Validation results for LEWICE 2.0. Technical Report CR 1999–208690, NASA, 1999.

Hao Xia and Paul G. Tucker. Finite volume distance field and its application to medial axis transforms. *International Journal for Numerical Methods in Engineering*, 82(1):114–134, 2010. ISSN 1097-0207. doi: 10.1002/nme.2762.

Chengxiang Zhu, Bin Fu, Zhiguo Sun, and Chunling Zhu. 3D ice accretion simulation for complex configuration basing on improved messinger model. In *International Journal of Modern Physics: Conference Series*, volume 19, pages 341–350. World Scientific, June 2012. doi: 10.1142/S2010194512008938.